Article

Label-Free Monitoring of Microorganisms and Their Responses to Antibiotics based on Self-Powered Microbead Sensors

Jhih-Cheng Wang, Shao-Wen Chi, Tai-Hua Yang, and Han-Sheng Chuang

ACS Sens., **Just Accepted Manuscript** • DOI: 10.1021/acssensors.8b00790 • Publication Date (Web): 17 Sep 2018

Label-Free Monitoring of Microorganisms and Their Responses to Antibiotics based on Self-Powered Microbead Sensors

Jhih-Cheng Wang[a,b], Shao-Wen Chi[a], Tai-Hua Yang[a,c,d], and Han-Sheng Chuang[a,d,*]

[a] *Department of Biomedical Engineering, National Cheng Kung University, Taiwan*

[b] *Department of Urology, Chimei Medical Center, Taiwan*

[c] *Department of Orthopedic Suegery, National Cheng Kung University Hospital, Taiwan*

[d] *Medical Device Innovation Center, National Cheng Kung University, Taiwan*

ABSTRACT

Rapid detection of bacteria and their susceptibility to specific antibiotics plays a vital role in microbial infection treatments. Antimicrobial susceptibility testing (AST) is a common measure to select effective drugs. However, the conventional practices, such as broth dilution, E-test, and disk diffusion, in clinical applications require a long turnaround time (~3 days), thereby compromising treatments and increasing mortality. This study presents self-powered sensors for on-site microorganism monitoring and rapid AST based on functionalized microbeads. The microbead sensors are driven by Brownian motion, rendering external power unnecessary. Fluorescent microbeads (d_p=2 μm) were coated with vancomycin to capture bacteria. The growth and responses of Gram-negative *Escherichia coli* and Gram-positive *Staphylococcus aureus* under antibiotic treatment were evaluated. The method showed stable selective binding despite the presence of some interferential substances, such as proteins and cells. Diffusivity change was strongly related to bacterial concentration. Accordingly, the diffusivity values of microbeads bound with motile and nonmotile bacteria exhibited specific paterns because of extra motility from microbes and increased

particle diameter. Only a drop of microbead–bacteria suspension (~5 μL) was needed in a microchip for each measurement. The microchip provided a steady environment for measurement over a few hours. By distinguishing the slope of the last four data points in the temporal diffusivity curve, bacterial susceptibility or resistance to specific antibiotics could be determined within a timeframe of 2 h. The study provides insights into saving more lives by using a fast and robust AST technique in future clinical practice.

***Keywords**: Antibiotic, Microbead, Brownian motion, Diffusometry, Biosensor, Bacteria*

Microbial infection is a leading cause of death worldwide[1]. Millions of patients with chronic diseases lost their lives because of these silent killers every year. To treat acute infections, clinical doctors should administer correct and effective antibiotics to patients in a timely manner. Antimicrobial susceptibility testing (AST) is a gold standard used nowadays to determine the suitable drugs and their minimum inhibitory concentrations (MICs). However, conventional methods, including broth dilution, E-test, and disk diffusion, usually require a long turnaround time (~3 days) because a minimum concentration of bacteria (10^7 cfu/mL) is required for visual observation.[2] To prevent life-threatening conditions and ease discomfort of patients, clinical doctors usually immediately administer "possible antibiotics" at a high dose to patients according to their experiences and clinical symptoms. Wrong guesses or overdose could lead to spread of superbugs or even death. Increased evidence released by the World Health Organization indicated possible depletion of our pharmaceutical arsenal if the use of antibiotics is mismanaged in the following decades. To cope with this concern, the demand for rapid AST is rising. Some technologies have been developed to tackle the lengthy process of microbial culture in AST. Multiplexed PCR[3-5] and an ultrafast DNA amplification, named digital real-time loop-mediated isothermal amplification,[6] are

capable of identifying drug-resistant bacteria from their genetic maps with only a minimal sample. Mass spectroscopy can even determine microbial species in a few minutes without tedious cell culture.[7-9] However, both methods are unable to determine the MICs for bacteria.

In recent years, numerous techniques to determine microbial susceptibility to antibiotics in a short turnaround time have been proposed. For example, magnetic beads have been widely applied to detect microbes.[10-14] Kinnunen et al.[15] reported a novel sensing technique based on asynchronous magnetic bead rotation (AMBR) to monitor the growth and drug susceptibility of individual bacteria. Single *Escherichia coli* cells were attached to magnetic beads via immunoreaction. The rotation period of a magnetic bead was found related to the growth of *E. coli* attached to it. The AST result could be determined within approximately 2 h. The size sensitivity of the AMBR sensor is as small as 80 nm. With a multiplexed microfluidic platform, Mohan et al.[16] achieved rapid AST within 2–4 h by detecting fluorescent intensity from stained *E. coli* mixed with antibiotics under an inverted microscope. Only 6 μL of sample was needed in the measurement, and nearly single cell sensitivity was reached. Thereafter, Choi et al.[17] developed an agarose microfluidic channel system to track single bacterial cells. *E. coli*, *Staphylococcus aureus*, and *Pseudomonas aeruginosa* were selected for the evaluation. All bacteria were immobilized on agarose with different antibiotic culture conditions. Their growth images were also recorded under a microscope. Eventually, the MIC values were obtained within 3–4 h. Recently, Sabhachandani et al.[18] have employed a similar concept of miniaturizing microbial testing with microfluidics. They developed a bead-based biosensor on an integrated microfluidic platform to carry out rapid AST. In their system, dilute *E. coli* concentration of 5×10^4 cfu/mL in a urine sample was successfully conducted for AST in an hour. Despite the significant reduction in turnaround time, most of the abovementioned rapid AST techniques rely on bacterial straining or observation of single functional particles.

For easy access to rapid AST without laborious preprocessing or heavy dependence on external instruments, we hereby propose label-free bead-based sensors to monitor microbial activities

and their responses to antibiotics (Fig. 1). In principle, microbeads bound with several bacteria express compromised Brownian motion and vice versa. This tendency is in good agreement with the number of bacteria in the medium. The activities and changes of functionalized beads are complex consequences of interactions among beads, bacteria, and random thermal movement. In our past studies,[19-20] the temporal diffusivity change reflects the growth condition of specific bacteria in the medium through immunoassays. Unfortunately, the immunoassay cannot proceed without bacterial species being identified in a clinical practice. For more practical applications, microbeads were coated with vancomycin instead of bacterial antibody in this study. Bacteria then bind to the microbeads via the hydrogen bonds between the vancomycin and D-Ala-D-Ala ligases on the bacterial cell walls[21-22]. However, the D-Ala-D-Ala ligases are covered with an extra layer of outer membrane in Gram-negative bacteria. The outer membrane protects Gram-negative bacteria from being targeted by some antibiotics like vancomycin. Nevertheless, prior study has found that the binding sites are likely to expose to the outside environment because of defects.[10] Accordingly, the binding between Gram-negative bacteria and vancomycin remains possible but lower in efficiency. Given that the binding is specific to bacteria only, the diffusivity changes in strong association with the bacterial concentration. A microchip was designed to enable the long-term imaging recording. With constant flipping, sedimentation was mitigated. Gram-negative *E. coli* and Gram-positive *S. aureus* were used in the study. The diffusivity of microbeads declined as the concentrations of both bacteria were increased. When a bacterial medium was mixed with gentamicin in accordance with the MIC values from the Clinical and Laboratory Standards Institute (CLSI) protocol, both showed good coincidence. The assessment suggests that the AST result could be determined within 2 h by using the proposed method. At last, an empirical criterion based on the slope of data was developed to enable future automation. The study provides insights into saving more lives by using a fast and robust AST technique in future clinical practice.

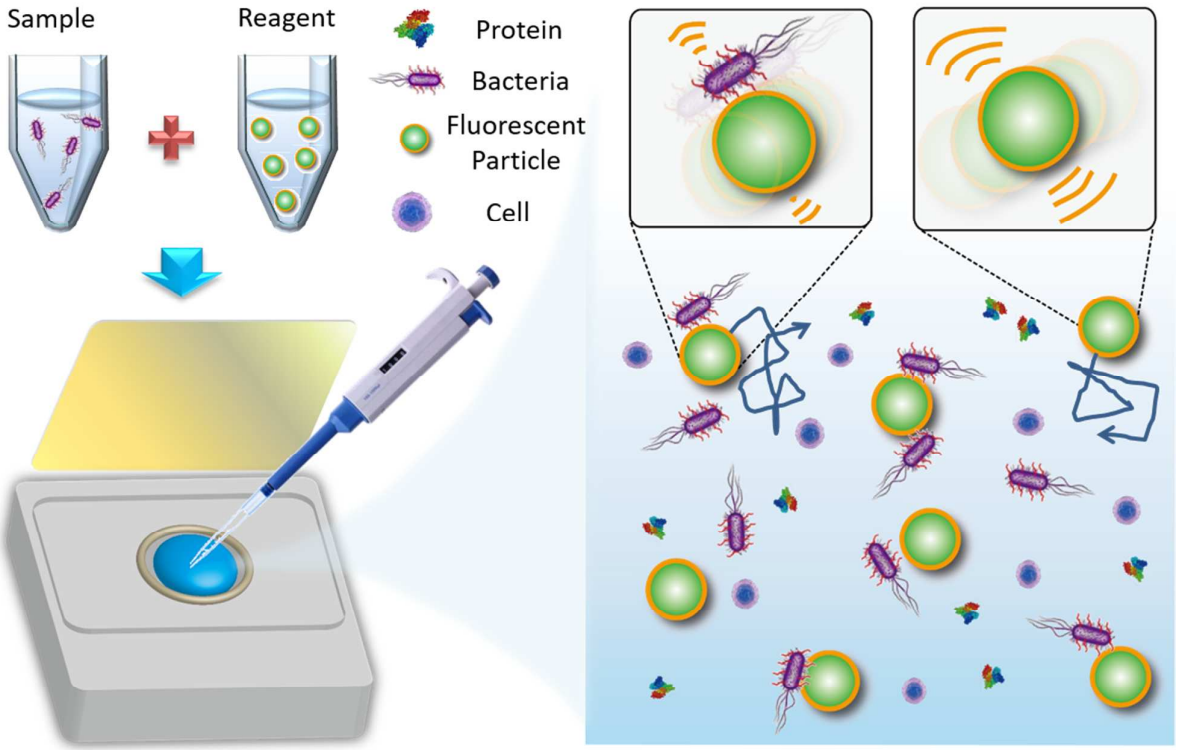

Fig. 1. Schematic of the self-powered microbead sensors for monitoring of live microorganisms (left). Theoretical concept of diffusivity changes between functionalized microbeads with and without bacteria attached (right). In general, micrbeads bound with bacteria express weaker Brownian motion.

■ MATERIALS AND METHODS

Experimental Setup and Microchip Fabrication

The bead-based sensors are self-powered by Brownian motion. Therefore, only a fluorescent microscope is needed to capture the consecutive images for analysis (Fig. 2A). In the study, an inverted epifluorescent microscope (OLYMPUS, IX71) equipped with a green-fluorescent-protein filter cube (OLYMPUS, U-MWIB3) and a 10× objective was used. A digital camera (FL3-U3-1382C-C8, Point Gray Research Inc.) was used to record images of each data for 20 s at a frame rate of 10 Hz. The overall lab temperature was maintained at 20 °C. The uncertainty was estimated below 0.6% when the temperature variation was within ±1 °C.

Microbial sample droplets were confined in a poly(methyl methacrylate) (PMMA) microchip for measurement (Fig. 2B). The microchip was fabricated by a computer numerical control machine (EGX-400, Roland). A depressed pedestal provides a space to position the samples. An O-ring and a cover glass were then used to seal the droplet to prevent evaporation. As shown in Fig. 2C, the major dimensions of the microchip are H=700 μm, h=460 μm, Φ_i=6.3 mm, and Φ_o=78 mm. A 2% bovine serum albumin solution was coated on the top cover glass and the bottom PMMA pedestal to prevent particles from surface adhesion. The microchip was also flipped every 2 min during measurement.

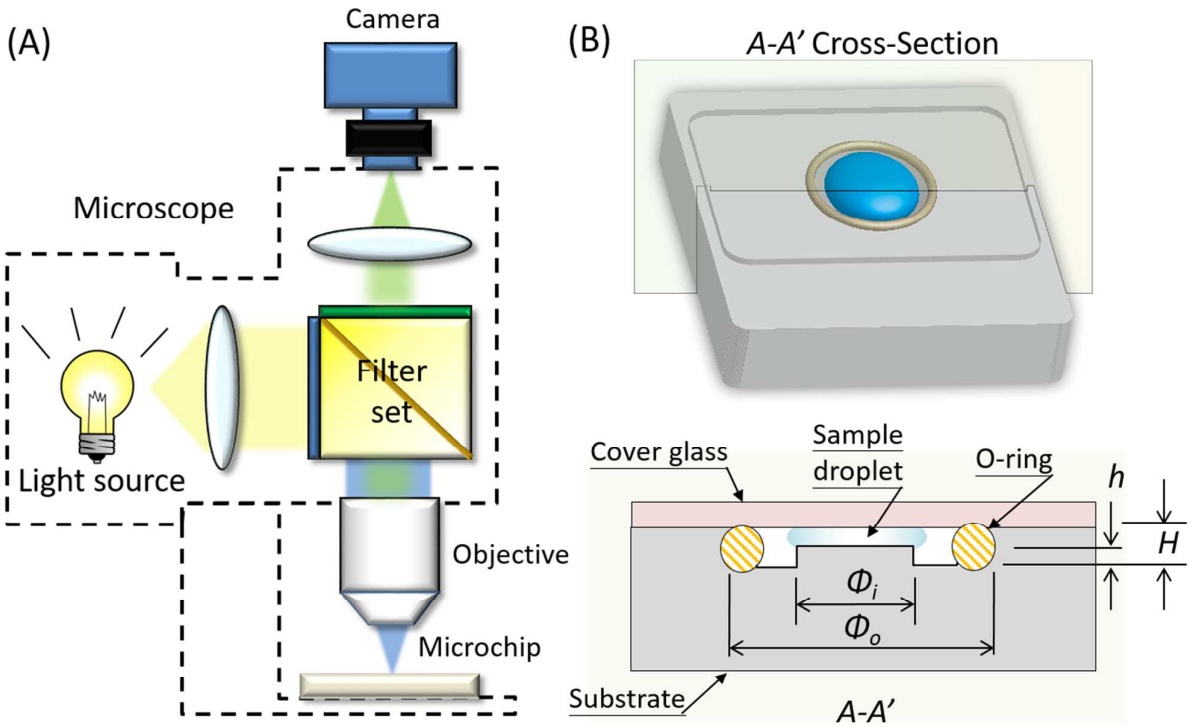

Fig. 2. (A) Schematic of the experimental setup. The measurement system is composed of a fluorescent microscope, a digital color camera connected to a computer, and a microchip. (B) The microchip contains a drop of sample sandwiched between a glass slide and the PMMA substrate. The dimensions of the microchip are clearly annotated in the A-A' cross section.

Bacterial Culture

E. coli (ATCC 25922), a Gram-negative motile bacterial strain (0.5–1×1.5–3 μm), and *S.*

aureus (ATCC 23360), a Gram-positive nonmotile bacterial strain (Φ=1–2 μm), were provided by Dr. H.C. Chang's laboratory in the Department of Biomedical Engineering at Nation Cheng Kung University, Taiwan. We took the frozen bacteria from a −80 °C freezer and mixed it with 30 mg/mL tryptic soy broth (211825-500g, BD). Both bacteria were incubated in a shaker at 37 °C for 12–16 h before use. The bacterial growth was examined under a microscope before each measurement. When conducting AST, the initial number of bacteria was adjusted with lysogeny broth (L2542, Sigma Aldrich) to approximately 10^6 cfu/mL. Gentamicin (G1264-1G, Sigma Aldrich) was mixed with a drop of bacterial solution to achieve the final concentration of 0–4 μg/mL. Gentamicin, an antibiotic widely known for inhibiting the synthesis of bacterial cell walls, was used to suppress the growth of *E. coli* and *S. aureus* in this study.

Preparation of Functionalized Microbeads

Vancomycin solution (B1507-1G, BioVision) was mixed with 10 mg/mL 1-ETHYL-3-(3-DIMETHYLAMINOPROPYL)-CARBODIIMIDE (EDC) and 10 mg/mL N-HYDROXYSUCCINIMIDE (NHS) for 15 min to activate the carboxylate groups. Then, amine-modified polystyrene fluorescent microbeads (d_p=2 μm; L4530, L9529, or L3030; Sigma-Aldrich) were first washed with phosphate-buffered saline with Tween-20 (PBST) to prevent aggregation, followed by incubation with 5 μL of the activated vancomycin solution at 4 ℃ and 800 rpm for 4 h. The final volumetric concentration was 0.568% v/v. The colloidal suspension was washed with PBST by centrifugation five times to remove freely suspending vancomycin. Notably, vancomycin is an antibiotic used in treating infections. By taking advantage of its strong affinity to the D-Ala-D-Ala binding sites of bacterial cell walls, the functional coating selectively attached to the bacteria but ignored proteins and normal cells. The selectivity allows vancomycin-functionalized microbeads to respond to only the bacteria. The microbeads were used as biosensors to detect the bacterial concentration in a sample suspension. For reference microbeads, amine-modified polystyrene fluorescent microbeads (d_p=2 μm; L4530, L9529, or L3030; Sigma-Aldrich) were

activated by 10 mg/mL EDC and 10 mg/mL NHS in the shaker at 800 rpm and 25 °C for 15 min. Subsequently, anti-tumor necrosis factor (TNF)-α was mixed with the suspension at 4 °C and 800 rpm for 4 h. Both functionalized microbeads were then incubated with the bacteria in a shaker at 37 °C for 1 h before measurement.

Our study indicated that the optimal particle diameter should be close to the size of the bacteria. A large bead size reduces sensitivity. By contrast, a small bead size results in a narrow measurement range. Considering the normal sizes of most bacteria range from submicrons to microns,[23-25] we determined the particle diameter to be 2 μm. In addition to the functionalized microbeads, reference microbeads were also needed in a complex medium to provide background fluctuations.

Determination of Diffusivity from Serial Images

Instead of monitoring bacteria by labeling them with fluorescent dyes,[26-27] the bacterial activity was monitored using the functionalized bead sensors. As a result, the pathogenic samples need less preprocessing steps and could be measured in a timely manner. Given that the particulate motion in static liquid is dominated by Brownian motion, diffusivity can provide quantitative information in relation to the change in bead size. In an unlimited 3D space, the diffusivity of a sphere can be well interpreted by the Stokes–Einstein relation.[28] In theory, the diffusivity is inversely proportional to the particle diameter when temperature and liquid viscosity are maintained constant. By contrast, the diffusivity is compromised when microbeads are in a confined space, a.k.a. hindered diffusion.[29] To control the hindered diffusion below 2%, our calculation showed that microbeads should maintain a distance of at least 28 μm away from the boundary.[30] Therefore, the particle images were only acquired from the middle plane of the microchip.

Notably, the Stokes–Einstein relation is suitable only for spherical particles. Single particles with irregular shapes induce bias in diffusion. Although the original microbeads are spherical, they

become irregular after attaching to bacteria. In other words, conventional particle tracking may not be able to show the true condition of particle motion in the medium. Alternatively, a statistical algorithm, termed spatial cross-correlation, was adopted herein to display a representative analysis. Our previous studies[19-20, 31] showed that the experimental data agree with the theoretical predictions. In general, few aggregates do not affect the overall correctness. Moreover, special care is needed in dealing with the measurement of motile bacteria. The bacterial motility counteracts the Stokes–Einstein relation because of extra energy. However, the diffusivity rise reverses at a critical time point as numerous bacteria are reproduced in the medium. To avoid misinterpretations, reference microbeads were required in the medium to provide background fluctuations. To this end, the diffusivity value of functionalized microbeads was divided by that of reference microbeads to yield relative diffusivity. Notably, this processing also improved the uncertainty due to thermal effect (see Supporting Information).

■ RESULTS AND DISCUSSION

Assessments of Microchip

For monitoring the activity of bacteria and their responses to antibiotics, bacteria should be incubated in an aqueous environment for hours. To this end, an additional O-ring dipped with mineral oil was installed in the microchip to reduce evaporation. Compared with the control (without O-ring) that dries out in 2 h, the sealed well in the microchip can retain a sample volume at 98% in 2 h and nearly 80% for 2 weeks under room temperature (Fig. 3A). Given that each AST test needs only 2 h for measurement, the reconfigured microchip was proven eligible for long-term monitoring.

Although the specific weight of the microbeads was close to the sample medium in the study, microbeads still slowly deposited to the bottom of the droplet. Regularly flipping the microchip improved the sedimentation (Fig. 3B). However, particle adhesion can be further reduced with the antifouling coating, bovine serum albumin (BSA), on the wall surfaces (Fig. 3B). Although

frequently flipping the microchip produced the best outcome, a compromised frequency of 2 min^{-1} was chosen due to the great amount of processing time needed.

Growth of *E. coli* and *S. aureus* was also observed in the microchip for 2 h to evaluate their growth states in a confined space (Figs. 3C and 3D). Each bacterial strain was measured under three conditions, namely, control (no antibiotic), growth with ineffective antibiotic (<2 μg/mL), and growth with effective antibiotic (>4 μg/mL). The bacteria under the control condition grew faster than those under the other conditions. The numbers of bacteria were double in *S. aureus* and nearly septuple in *E. coli*. According to the CLSI protocol, the MICs for *E. coli* and *S. aureus* were 4 and 2 μg/mL, respectively. Therefore, a drug concentration less than 2 μg/mL was insufficient to inhibit the growth of both bacteria. However, compared with the growth with an effective drug concentration, the high slopes imply that the bacteria in the microchip were not completely eliminated by the antibiotics. As a result, the bacteria showed slow growth because they were partially inhibited by the ineffective drug. The results eventually suggest that the microchip is feasible for the detection of live bacteria.

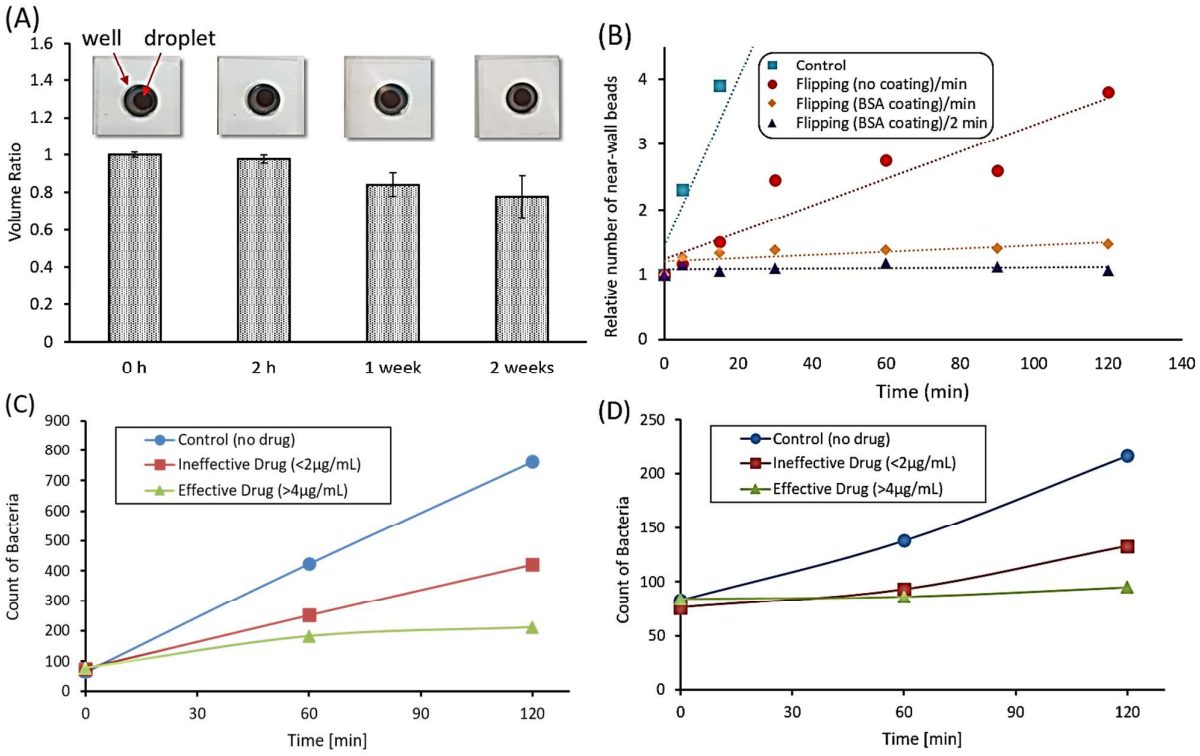

Fig. 3. (A) Measurement of sample volume ratio in the microchip due to evaporation over two weeks. The microchip was maintained at room temperature (n=3). (B) Effect of microbead adhesion on the channel walls in flipping microchips. (C) Growth of *E. coli* in a microchip over 2 h. (D) Growth of *S. aureus* in a microchip over 2 h.

Interactions between Microbeads and Bacteria

Unlike the specific binding in immunoreactions, the binding forces between vancomycin and bacterial cell walls are more universal and rely on hydrogen bonds (Fig. 4A). Vancomycin is a β-lactam antibiotic that possesses a similar structure to DD-transpeptidase, an enzyme that catalyzes the synthesis of bacterial cell walls. Almost all bacteria have cell walls with D-Ala-D-Ala residues. Although Gram-negative bacteria are covered with an extra layer of outer membrane, the D-Ala-D-Ala ligases still can expose to the outside environment through some defects.[10] Therefore, the vancomycin coating can selectively capture most bacteria instead of normal cells or proteins. Notably, vancomycin only affected those bacteria attached to microbeads by inhibiting their wall

synthesis. For free swimmers, however, no significant influence was ever found. Actually, the antibiotic inhibition benefited the evaluation of diffusivity because inhibited bacteria behaved more like dead cells, leaving their Brownian motion similar to our predicted model.

Successfully functionalizing microbeads with vancomycin was the first step to achieve the monitoring of bacteria in the medium. Fourier transform infrared (FTIR) spectroscopy (FTIR-4600, JASCO) was performed to verify the coating on the microbeads (Fig. 4B). After washing the colloidal suspension thrice to remove the unstable adsorption of vancomycin on the microbead surfaces, we observed the characteristic peaks of vancomycin at 1634 cm^{-1} due to amide I band and a broad absorption band centered at 3334 cm^{-1} due to amide A band superposition originating from N–H stretching vibrations with bands from O–H stretches and overtones from C=O stretching vibrations (Fig. 4B). The peaks in the FTIR spectrum provide a direct evidence of successful coating of vancomycin on the microbeads. The functionalized microbeads were then used to check their binding effects with bacteria, cells, and BSA proteins. A series of bright field images over a timeframe of 2 h showed increased clusters of bacteria progressively attached to the tracked microbeads (Fig. 4C). In the presence of BSA proteins, the binding efficacy was not significantly compromised. A thorough statistical investigation of the binding efficacies with different sources is listed in Table 1. Vancomycin showed universal affinity with all three bacteria among other functional coatings. Surprisingly, pure polystyrene microbeads, amine-modified, and carboxylate-modified microbeads were all also capable of attaching to the bacteria despite the low efficacies. Only the antibody coating was free from binding with any bacteria. Notably, the presence of BSA and cells in the medium did not interfere with the binding efficacy between the bacteria and the microbeads. Therefore, the evaluation suggests that vancomycin is an ideal functional coating in selectively binding with bacteria. By contrast, anti-TNF-α was coated on reference microbeads to prevent the bead surfaces from bacteria, cells, and proteins.

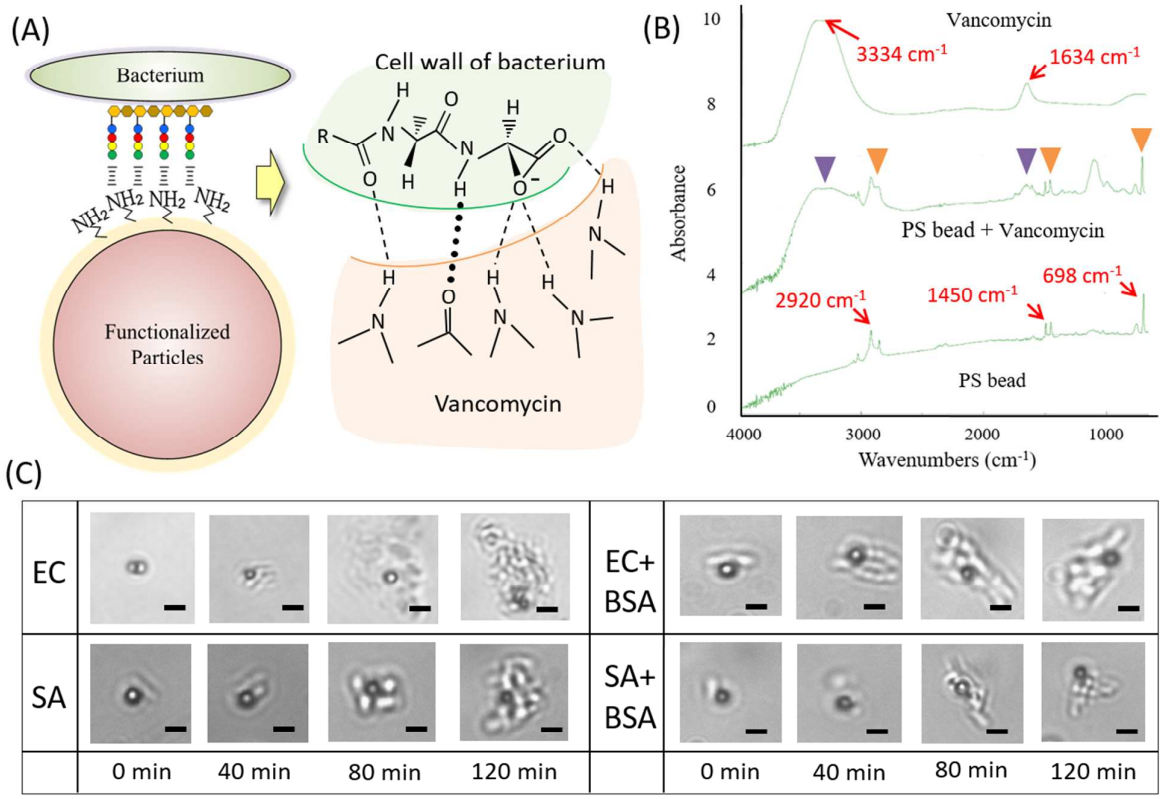

Fig. 4. (A) Illustration of binding mechanism between bacterial cell wall and vancomycin coating. (B) FTIR spectrums of the PS microbead, vancomycin, and PS microbead coated with vancomycin. (C) Growth evolutions of *E. coli* (EC) and *S. aureus* (SA) over 2 h. The growth is not disturbed in the presence of BSA. The scale bars denote 5 μm.

Table 1. Binding efficacy between functionalized microbeads and different bacteria strains in a complex medium.

	Bacteria attached to microbeads (%)							
	Amine	None	Carboxylate	Anti-TNF-α	Vancomycin (5×10^6 cfu/mL)	Vancomycin +BSA	Vancomycin +Cells	Vancomycin +BSA +Cells
S. aureus	12.6%	85.2%	77.4%	0	70%	68.8%	65.5%	73.2%
E. coli	13%	26.6%	9.2%	0	40.3%	41.2%	43.1%	41.3%

Stability of Microbead Sensors

Stability of the microbead sensors was investigated. Pure microbead suspension without functional coatings or bacteria attached was measured every 20 min over a timeframe of 2 h (Fig. 5A). With the lab temperature maintained constant, the standard deviation of temporal variation was less than 2.8%. In addition, five microchips with the same pure microbead suspension were measured (Fig. 5B). The standard deviation of reproducibility between microchips was less than 1.9%. Both results suggest great stability of the technique in time and between items.

Effect of Diffusivity and Number of Bacteria

A range of bacterial concentrations, 10^4–10^9 cfu/mL, was investigated for the relationship between diffusivity and the number of bacteria. To avoid undesirable disturbances resulting from the motile bacteria, all bacteria were sterilized by UV light for 24 h in advance. To ensure the binding between microbeads and that the bacteria were complete and stable, we conducted the measurement after the incubation of functionalized microbeads and bacteria.

For each data point, 200 consecutive images were recorded to alleviate uncertainty. The relative diffusivity was derived by dividing the experimental group by the reference group to obtain only the influence of bacteria attached to the microbeads. Four experimental groups were measured to study how their concentrations alter the diffusivity values according to different bacterial compositions. The four groups include two pure bacterial strains (*E. coli* and *S. aureus*) and two mixed bacterial strains (30% *E. coli*+70% *S. aureus* and 70% *E. coli*+30% *S. aureus*). A fairly linear relationship was observed between the relative diffusivity and the bacterial concentration (Fig. 5C). In addition, the diffusivity values of the measured samples were not seriously altered by the bacterial compositions. Notably, the diffusivity change turned ambiguous when the bacterial concentration was less than 10^4 cfu/mL.[19] The change became distinguishable after the bacterial concentration exceeded the threshold. The blank determination method was used here for the limit of detection

(LOD) determination. Specifically, LOD was determined at the intersection point between the trend line of the bacterial concentration and the control value plus three standard deviations (1.05±0.11). Accordingly, the LOD of this technique was estimated to be nearly 10^5 cfu/mL.

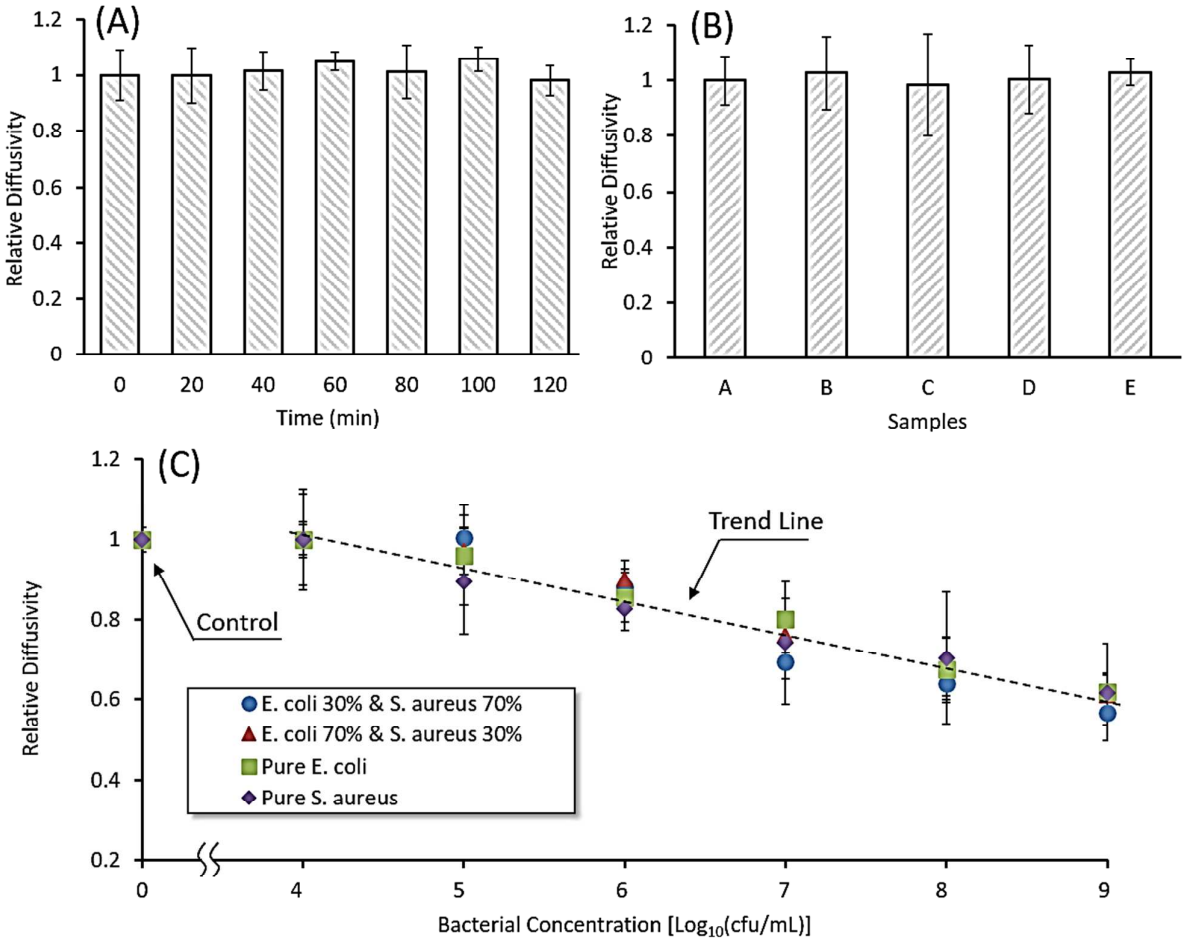

Fig. 5. (A) Temporal stability and (B) reproducibility of the microbead sensing technique (n=5). (C) Relative diffusivity changes with respect to bacterial concentration ranging from 10^4 cfu/mL to 10^9 cfu/mL. The bacteria were sterilized with UV for 24 h before measurement. Four bacterial compositions were evaluated. The error bars represent standard errors (n≥5).

Evaluations of Rapid Antimicrobial Susceptibility Testing

A complete AST evaluation of this technique requires monitoring the activity of bacteria for a period of time (~2 h). Bacteria and the functionalized microbeads were incubated in the microchip simultaneously (Movies S1 and S2). The MICs of gentamicin for the *E. coli* and *S. aureus* strains were respectively 4 and 2 μg/mL in accordance with the CLSI protocol. Considering that bacteria usually reproduce every 20 min, we measured data points from the beginning to 2 h every 20 min. Temporal diffusivity changes were sketched to display the growth activities of bacteria under the applied conditions (Figs. 6A and 6B). For convenient determination, the drug susceptibility was simply expressed in terms of the slope of the last four data points in the study (see Supporting Information). In general, a positive value or a level slope could represent effective drugs. However, a negative value might link to failure. According to the regression lines that fit the last four data points, all the control groups show negative slopes (-0.0044/min for *E. coli* and -0.0033/min for *S. aureus*) while *E. coli* and *S. aureus* with effective antibiotics show positive slopes of 0.0055/min and 0.0005/min, respectively. The results imply that both *E. coli* and *S. aureus* continuously reproduced and accumulated around the vancomycin-functionalized microbeads within 2 h in the absence of gentamicin. The microbeads bound with either *E. coli* or *S. aureus* exhibited declining diffusivity trends during the entire measurement. Our previous study indicated that two major factors, bacterial motility and equivalent particle diameter, directly contribute to the Brownian motion of microbeads. In the presence of motile bacteria, bacterial motility dominates the diffusivity, resulting in a rise in the very beginning (roughly 20–40 min) [19]. Subsequently, several bacterial clusters attached to microbeads progressively drag down the diffusivity. Nonetheless, no evident rise was observed in the figure because the *E. coli* here was low in concentration and expressed compromised motility. In the presence of nonmotile bacteria, however, the diffusivity declined monotonically in 2 h only with the increased equivalent particle diameter. By contrast, when effective antibiotics were added into the bacterial suspensions, the declining trends in both motile and nonmotile bacteria were all ceased at

certain time points. Although the mean diffusivity values formed meaningful trends, some of their standard errors were large. The variation could be attributed to the inhomogeneous distribution of microbeads resulting from sedimentation. A short time gap between measurements and an increased number of measurement will be considered for future improvement.

Reference microbeads were measured simultaneously to rule out the background noise. Thus, only interactions between the microbeads and bacteria were considered (Fig. 6C). When an effective concentration of gentamicin was mixed with the bacterial suspension, the growth of both bacteria was inhibited at a certain time point. Accordingly, the temporal diffusivity curve was altered after that particular point. The diffusivity also stopped declining and then maintained its level because the bacterial activity was ceased. Meanwhile, the temporal diffusivity curve was in accordance with the previous condition without antibiotic in the presence of an ineffective concentration of gentamicin. The results suggest that the effectiveness of antibiotics can be determined by the tendency of the diffusivity data after the turning point. A declining diffusivity, i.e., a negative slope, indicates failure of antibiotics and vice versa (Fig. 6D). The turning point may imply the moment that the drug started to take effect.

Notably, microbead aggregation occasionally occurred when microbeads collided to each other frequently because of inhomogeneous dispersion. Statistically, the degree of microbead aggregation escalated with the bacterial concentration. Although serious aggregation was unfavorable in the study, minor aggregation contributed to lowering the diffusivity. In fact, the cross-correlation algorithm is inherently a measure of statistical analysis and is thus capable of mitigating the bias resulting from the aggregation. As a result, our overall measurement was able to resist interferences from slight microbead aggregation.

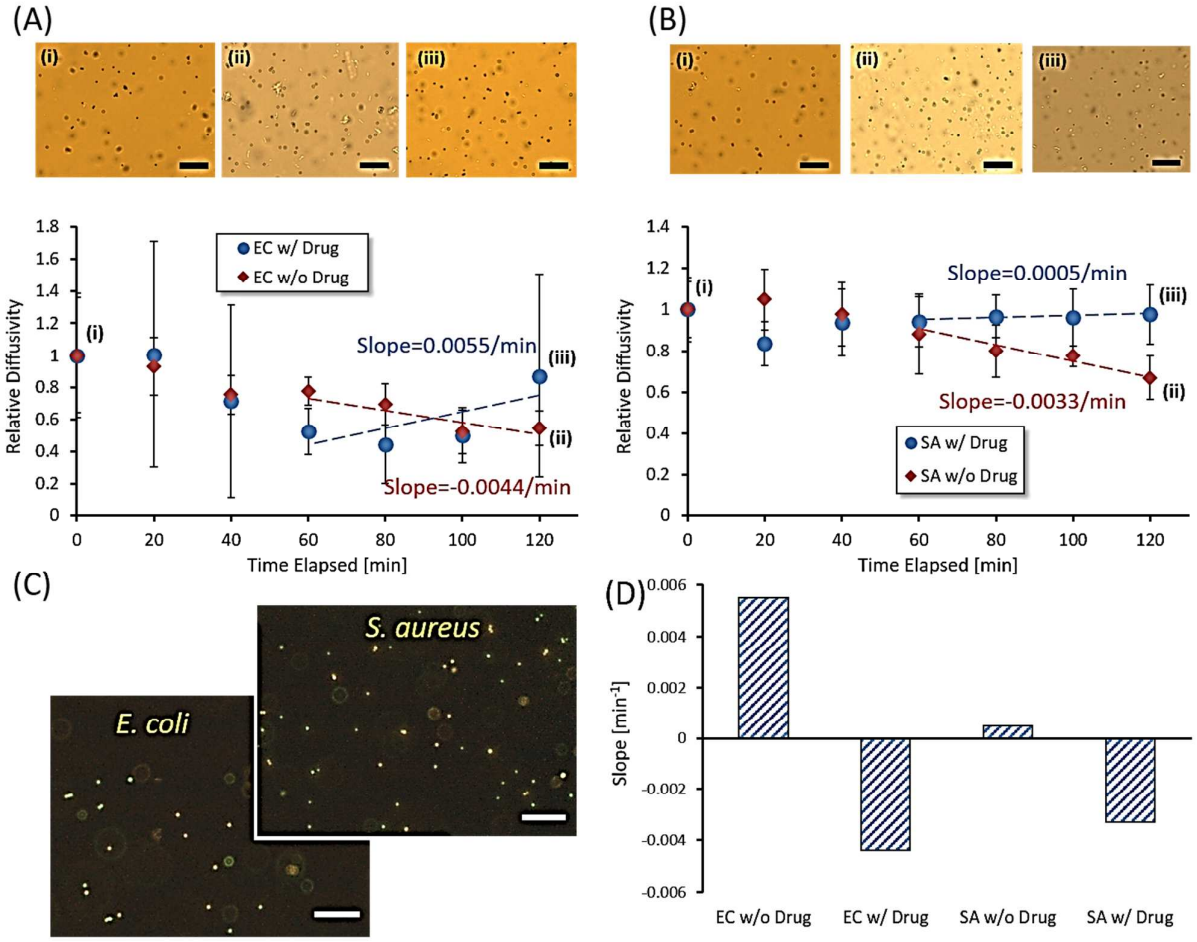

Fig. 6. (A) Temporal diffusivity change over a timeframe of 2 h (n=5). The blue circles and red diamonds represent *E. coli* with and without effective gentamicin (4 μm/mL), respectively. The error bars represent standard errors. The insets are bright-field images recorded at different time points. The scale bar is 20 μm. (B) Temporal diffusivity change over a timeframe of 2 h (n=6). The blue circles and red diamonds represent *S. aureus* with and without effective gentamicin (2 μm/mL), respectively. The error bars represent standard errors. The insets are bright-field images recorded at different time points. The scale bar is 20 μm. (C) Raw images taken in the fluorescent mode. Orange microbeads represent the sensing probes and green microbeads represent references associated with the background fluctuations. The scale bar is 20 μm. (D) Effect of the rapid AST test, where a positive slope stands for an effective antibiotic on the inhibition of bacteria and vice versa. Both bacteria are sensitive to the drug concentrations used.

■ CONCLUSION

This study showcased a label-free bead-based diffusometry technique for the rapid, simple, and sensitive monitoring of microorganisms and AST. The vancomycin coating showed high selectivity to bacteria. This condition enabled specific monitoring of only bacteria rather than cells and proteins. In principle, Brownian motion is inversely proportional to the equivalent particle diameter if target bacteria are dead or nonmotile. Conversely, motile bacteria boost the diffusivity by imparting microbeads with additional energy. However, the increased particle diameter would lead to subsequent declination in microbead diffusivity when the bacterial population in a culture broth exceeded a sustainable threshold. In addition to the motility analysis, live and dead bacterial cells can be determined by looking into their diffusivity patterns. A rise in the initial phase of the diffusivity curve is strongly attributed to the extra energy from motile bacteria.

As a general criterion, the bacteria express drug susceptibility when the temporal diffusivity curve of the microbead–bacterium complexes displays a turning point during its declining phase. Otherwise, the bacteria were regarded resistant to the drug. Several concentrations of antibiotics were investigated for their sterilization effects. Our result explicitly indicated that 2 and 4 μg/mL gentamicin inhibited the growth of *S. aureus* and *E. coli*, respectively. Our findings are also in good agreement with the CLSI protocol.

Overall, a complete AST cycle was accomplished on the system within 2 h. In addition, the technique featured small sample volume (5 μL) and low LOD (~10^5 cfu/mL). The preliminary AST assessment in the study assured the practical use of the technique in the future clinical diagnosis.

■ ASSOCIATED CONTENT

Supporting Information

The Supporting Information is available free of charge on the ACS Publications website at DOI: ***/***.

Determination of AST in the study was dependent on the slope of the temporal diffusivity. In the 2-h measurement, seven data points of diffusivity were acquired to show the bacterial activity. Improvement of uncertainty due to thermal effect dealt with two steps to mitigate the thermal fluctuation, including room temperature control and addition of reference microbeads in the same medium.

■ AUTHOR INFORMATION

Corresponding Author

*E-mail: oswaldchuang@mail.ncku.edu.tw

ORCID

Han-Sheng Chuang: 0000-0002-7257-6565

Note

The authors declare no competing financial interest.

■ ACKNOWLEDGMENTS

This research was supported by the Ministry of Science and Technology under the grant numbers 104-2221-E-006 -054 -MY3 and 107-2622-E-006-022 –CC2. We appreciate Dr. H.C. Chang for his kind share of *E. coli* and *S. aureus*. Moreover, C. C. Wang and T.H. Yang would also like to thank Chimei Medical Center for the grant CMNCKU10720.

■ REFERENCES

1. Lever, A.; Mackenzie, I., Sepsis: definition, epidemiology, and diagnosis. *BMJ* **2007,** *335* (7625), 879-883.

2. Reller, L. B.; Weinstein, M.; Jorgensen, J. H.; Ferraro, M. J., Antimicrobial susceptibility testing: A review of general principles and contemporary practices. *Clin. Infect. Dis.* **2009,** *49* (11), 1749-1755.

3. Rathore, K.; Joseph, B.; Sharma, D. K.; Gaurav, A.; Sharma, S. K.; Milind, M.; Patel, P.; Prakash, C.; Singh, L., Evaluation of multiplex polymerase chain reaction as an alternative to conventional antibiotic sensitivity test. *Veterinary World* **2018,** *11* (4), 474-479.

4. Ramachandran, D.; Bhanumathi, R.; Singh, D. V., Multiplex PCR for detection of antibiotic resistance genes and the SXT element: application in the characterization of Vibrio cholerae. *J. Med. Microbiol.* **2007,** *56* (3), 346-351.

5. Ali, R.; Al-Achkar, K.; Al-Mariri, A.; Safi, M., Role of Polymerase Chain Reaction (PCR) in the detection of antibiotic-resistant Staphylococcus aureus. *Egyptian Journal of Medical Human Genetics* **2014,** *15* (3), 293-298.

6. Schoepp, N. G.; Schlappi, T. S.; Curtis, M. S.; Butkovich, S. S.; Miller, S.; Humphries, R. M.; Ismagilov, R. F., Rapid pathogen-specific phenotypic antibiotic susceptibility testing using digital LAMP quantification in clinical samples. *Science Translational Medicine* **2017,** *9* (410).

7. Krásný, L.; Hynek, R.; Hochel, I., Identification of bacteria using mass spectrometry techniques. *Int. J. Mass Spectrom.* **2013,** *353*, 67-79.

8. Idelevich, E. A.; Sparbier, K.; Kostrzewa, M.; Becker, K., Rapid detection of antibiotic resistance by MALDI-TOF mass spectrometry using a novel direct-on-target microdroplet growth assay. *Clinical Microbiology and Infection* **2018,** *24* (7), 738-743.

9. Charretier, Y.; Schrenzel, J., Mass spectrometry methods for predicting antibiotic resistance. *PROTEOMICS – Clinical Applications* **2016,** *10* (9-10), 964-981.

10. Gu, H.; Xu, K.; Xu, C.; Xu, B., Biofunctional magnetic nanoparticles for protein separation and pathogen detection. *Chem. Comm.* **2006,** (9), 941-949.

11. Pappert, G.; Rieger, M.; Niessner, R.; Seidel, M., Immunomagnetic nanoparticle-based sandwich chemiluminescence-ELISA for the enrichment and quantification of E. coli. *Microchimica Acta* **2010,** *168* (1), 1-8.

12. Shen, Z.-Q.; Wang, J.-F.; Qiu, Z.-G.; Jin, M.; Wang, X.-W.; Chen, Z.-L.; Li, J.-W.; Cao, F.-H., QCM immunosensor detection of Escherichia coli O157:H7 based on beacon immunomagnetic nanoparticles and catalytic growth of colloidal gold. *Biosens. Bioelectron.* **2011,** *26* (7), 3376-3381.

13. Setterington, E. B.; Alocilja, E. C., Rapid electrochemical detection of polyaniline-labeled Escherichia coli O157:H7. *Biosens. Bioelectron.* **2011,** *26* (5), 2208-2214.

14. Lattuada, M.; Ren, Q.; Zuber, F.; Galli, M.; Bohmer, N.; Matter, M. T.; Wichser, A.; Bertazzo, S.; Pier, G. B.; Herrmann, I. K., Theranostic body fluid cleansing: rationally designed magnetic

particles enable capturing and detection of bacterial pathogens. *Journal of Materials Chemistry B* **2016,** *4* (44), 7080-7086.

15. Kinnunen, P.; Sinn, I.; McNaughton, B. H.; Newton, D. W.; Burns, M. A.; Kopelman, R., Monitoring the growth and drug susceptibility of individual bacteria using asynchronous magnetic bead rotation sensors. *Biosens. Bioelectron.* **2011,** *26* (5), 2751-2755.

16. Mohan, R.; Mukherjee, A.; Sevgen, S. E.; Sanpitakseree, C.; Lee, J.; Schroeder, C. M.; Kenis, P. J. A., A multiplexed microfluidic platform for rapid antibiotic susceptibility testing. *Biosens. Bioelectron.* **2013,** *49*, 118-125.

17. Choi, J.; Jung, Y.-G.; Kim, J.; Kim, S.; Jung, Y.; Na, H.; Kwon, S., Rapid antibiotic susceptibility testing by tracking single cell growth in a microfluidic agarose channel system. *Lab Chip* **2013,** *13* (2), 280-287.

18. Sabhachandani, P.; Sarkar, S.; Zucchi, P. C.; Whitfield, B. A.; Kirby, J. E.; Hirsch, E. B.; Konry, T., Integrated microfluidic platform for rapid antimicrobial susceptibility testing and bacterial growth analysis using bead-based biosensor via fluorescence imaging. *Microchimica Acta* **2017,** *184* (12), 4619-4628.

19. Chung, C.-Y.; Wang, J.-C.; Chuang, H.-S., Simultaneous and quantitative monitoring of co-cultured Pseudomonas aeruginosa and Staphylococcus aureus with antibiotics on a diffusometric platform. *Sci. Rep.* **2017,** *7*, 46336.

20. Chung, C.-Y.; Wang, J.-C.; Chuang, H.-S., Rapid Bead-Based Antimicrobial Susceptibility Testing by Optical Diffusometry. *PLOS ONE* **2016,** *11* (2), e0148864.

21. Kell, A. J.; Stewart, G.; Ryan, S.; Peytavi, R.; Boissinot, M.; Huletsky, A.; Bergeron, M. G.; Simard, B., Vancomycin-Modified Nanoparticles for Efficient Targeting and Preconcentration of Gram-Positive and Gram-Negative Bacteria. *ACS Nano* **2008,** *2* (9), 1777-1788.

22. Lin, Y.-S.; Tsai, P.-J.; Weng, M.-F.; Chen, Y.-C., Affinity Capture Using Vancomycin-Bound Magnetic Nanoparticles for the MALDI-MS Analysis of Bacteria. *Analytical Chemistry* **2005,** *77* (6), 1753-1760.

23. Velimirov, B., Nanobacteria, Ultramicrobacteria and Starvation Forms: A Search for the Smallest Metabolizing Bacterium. *Microbes and Environments* **2001,** *16* (2), 67-77.

24. Schulz, H. N.; Jørgensen, B. B., Big Bacteria. *Annu. Rev. Microbiol.* **2001,** *55* (1), 105-137.

25. Fischer, C. L.; Walters, K. S.; Drake, D. R.; Blanchette, D. R.; Dawson, D. V.; Brogden, K. A.; Wertz, P. W., Sphingoid bases are taken up by Escherichia coli and Staphylococcus aureus and induce ultrastructural damage. *Skin Pharmacol. Physiol.* **2013,** *26* (1), 36-44.

26. Anaya, C.; Church, N.; Lewis, J. P., Detection and identification of bacterial cell surface proteins by fluorescent labeling. *Proteomics* **2007,** *7* (2), 215-219.

27. Harkins, K. R.; Harrigan, K., Labeling of Bacterial Pathogens for Flow Cytometric Detection and Enumeration. *Curr. Protoc. Cytom.* **2004,** *29* (1), 11.17.1-11.17.20.

28. Einstein, A.; Fürth, R., *Investigations on the theory of Brownian movement*. Dover Publications: New York, N.Y., 1956.

29. Huang, P.; Breuer, K. S., Direct measurement of anisotropic near-wall hindered diffusion using total internal reflection velocimetry. *Phys. Rev. E* **2007,** *76* (4), 046307.

30. Sie, Y.-S.; Chuang, H.-S., A micro-volume viscosity measurement technique based on μPIV diffusometry. *Microfluid. Nanofluid.* **2014,** *16* (1), 65-72.

31. Chuang, H.-S.; Chen, Y.-J.; Cheng, H.-P., Enhanced diffusometric immunosensing with grafted gold nanoparticles for detection of diabetic retinopathy biomarker tumor necrosis factor-α. *Biosens. Bioelectron.* **2018,** *101*, 75-83.

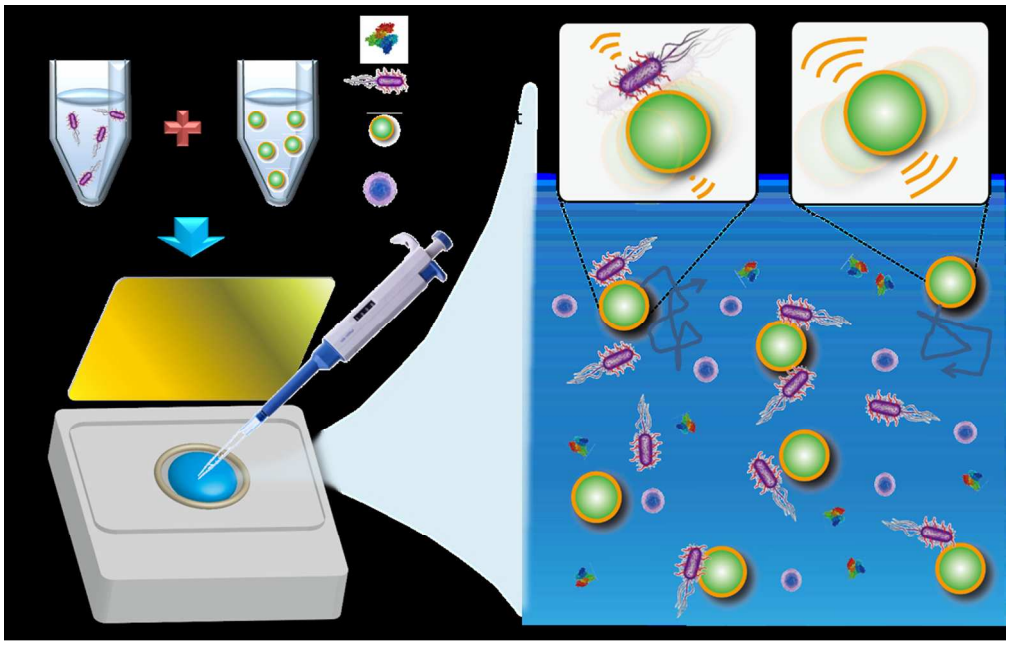

Schematic of the self-powered microbead sensors for monitoring of live microorganisms (left). Theoretical concept of diffusivity changes between functionalized microbeads with and without bacteria attached (right). In general, micrbeads bound with bacteria express weaker Brownian motion.

204x129mm (150 x 150 DPI)

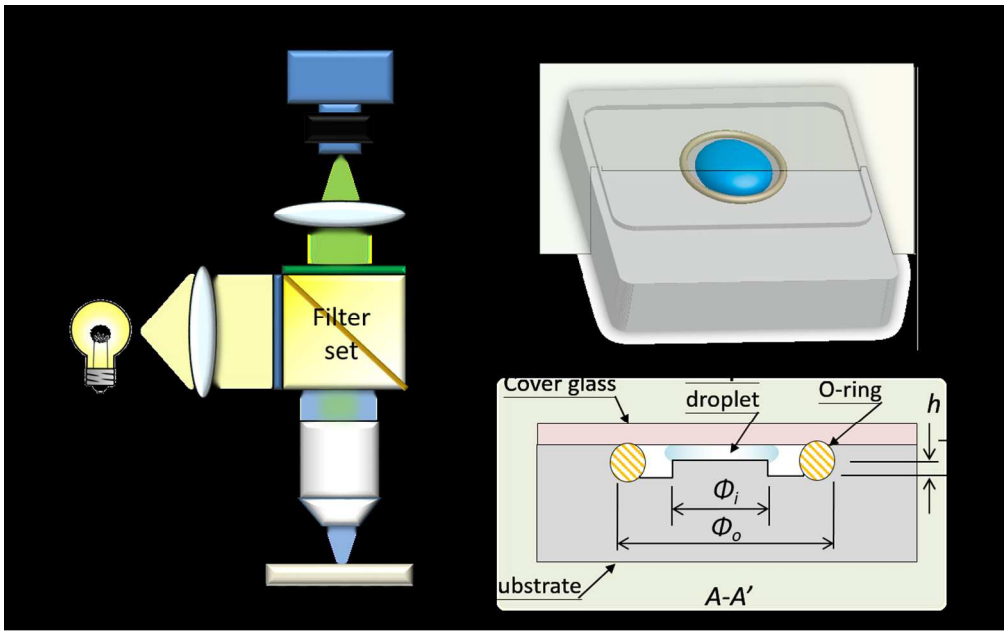

(A) Schematic of the experimental setup. The measurement system is composed of a fluorescent microscope, a digital color camera connected to a computer, and a microchip. (B) The microchip contains a drop of sample sandwiched between a glass slide and the PMMA substrate. The dimensions of the microchip are clearly annotated in the A-A' cross section.

226x141mm (150 x 150 DPI)

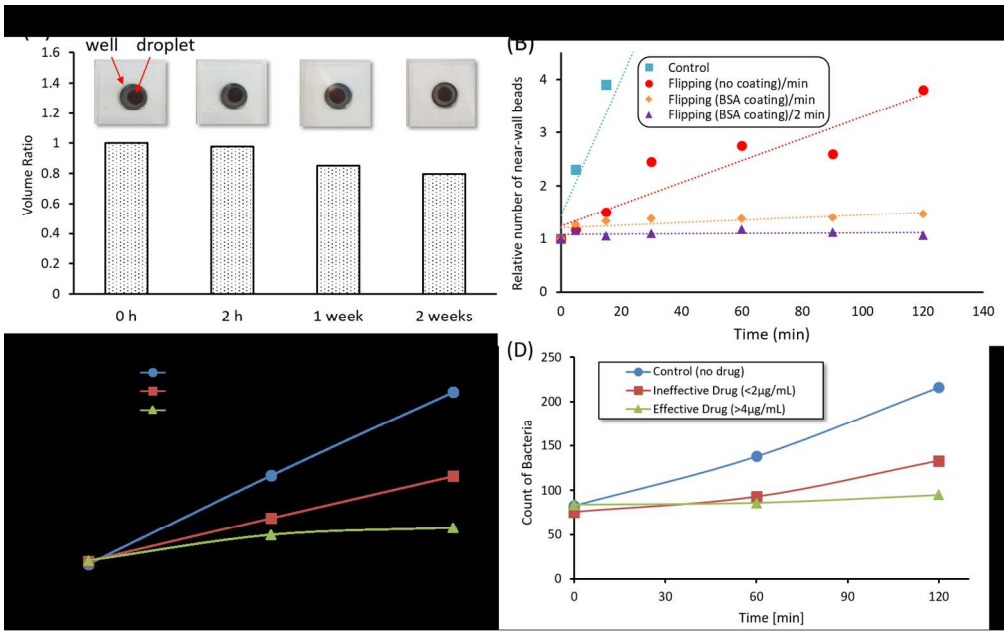

(A) Measurement of sample volume ratio in the microchip due to evaporation over two weeks. The microchip was maintained at a room temperature. (B) Effect of microbead adhesion on the channel walls in flipping microchips. (C) Growth of E. coli in a microchip over 2 h. (D) Growth of S. aureus in a microchip over 2 h.

284x177mm (150 x 150 DPI)

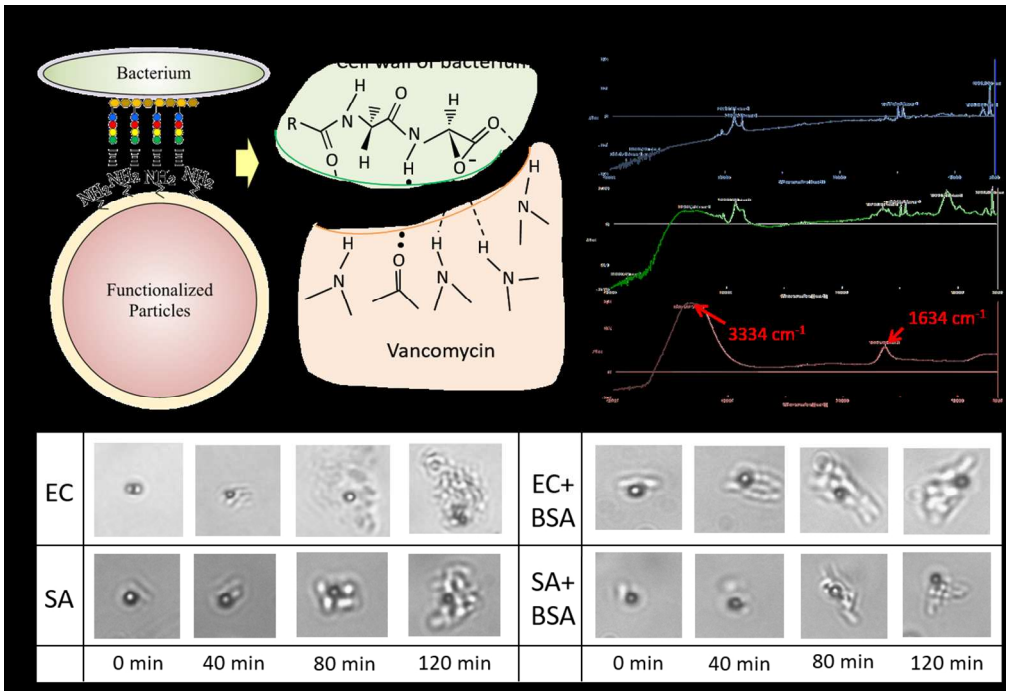

(A) Illustration of binding mechanism between bacterial cell wall and vancomycin coating. (B) FTIR spectrums of the PS microbead, vancomycin, and PS microbead coated with vancomycin. (C) Growth evolutions of E. coli (EC) and S. aureus (SA) over 2 h. The growth is not disturbed in the presence of BSA.

221x151mm (150 x 150 DPI)

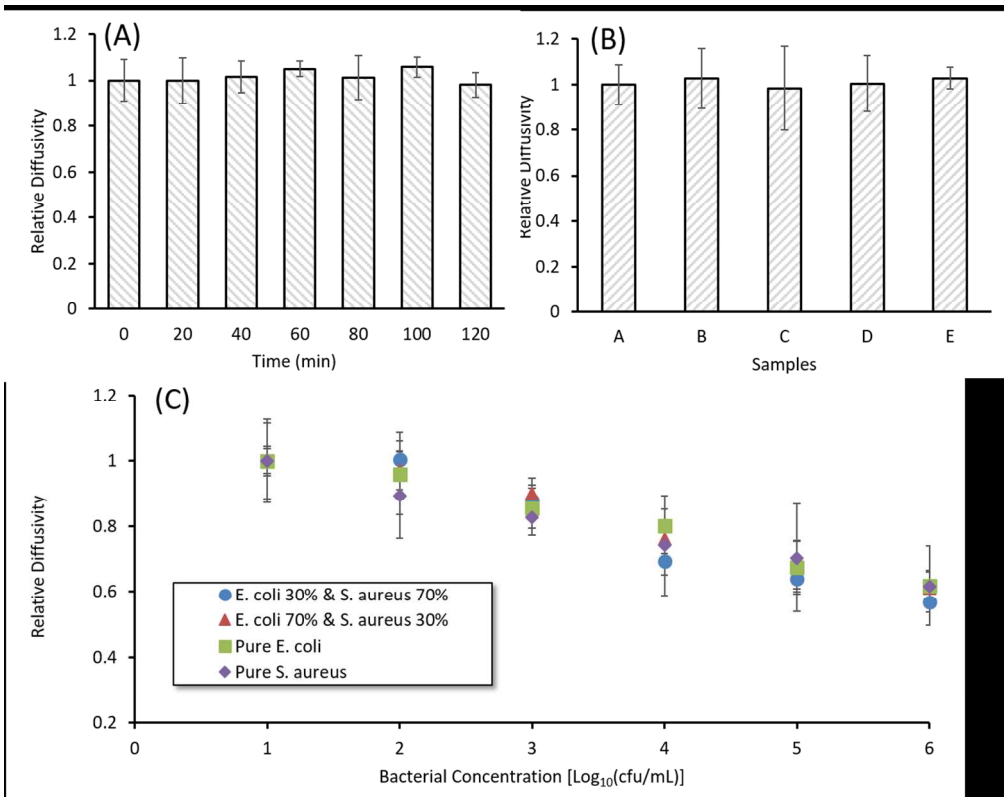

(A) Temporal stability and (B) reproducibility of the microbead sensing technique (n=5). (C) Relative diffusivity changes with respect to bacterial concentration ranging from 104 cfu/mL to 109 cfu/mL. The bacteria were sterilized with UV for 24 h before measurement. Four bacterial compositions were evaluated. The error bars represent standard errors (n≥5).

220x174mm (150 x 150 DPI)

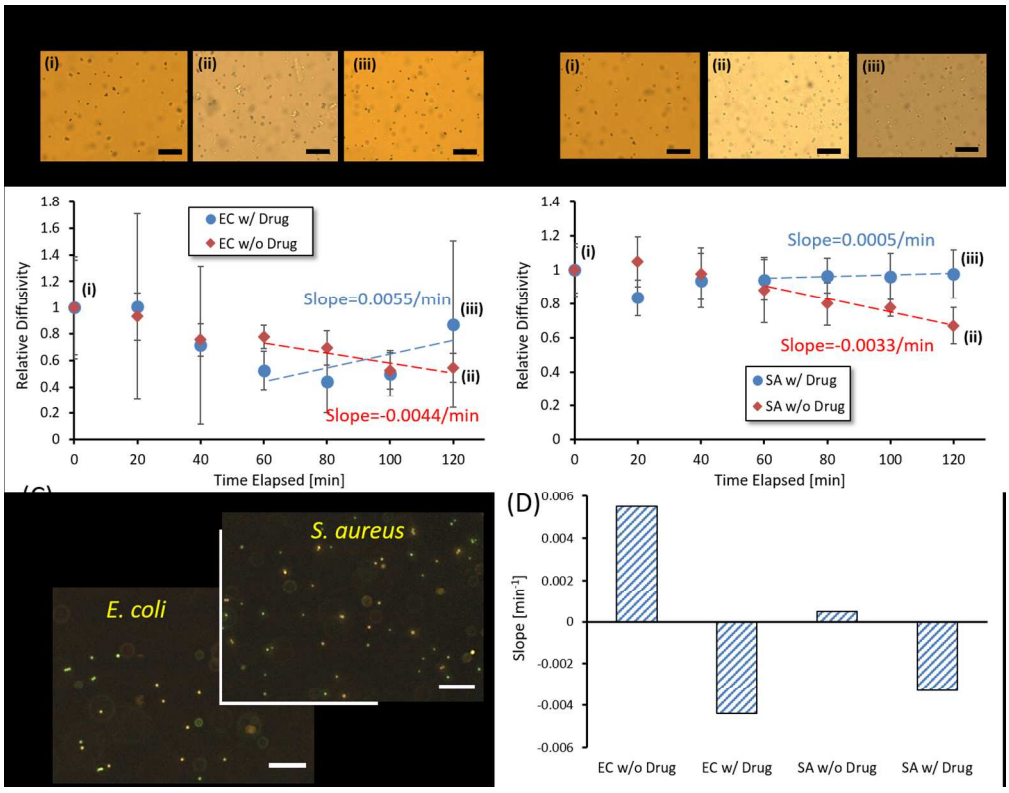

(A) Temporal diffusivity change over a timeframe of 2 h (n=5). The blue circles and red diamonds represent E. coli with and without effective gentamicin (4 μm/mL), respectively. The error bars represent standard errors. The insets are bright-field images recorded at different time points. The scale bar is 20 μm. (B) Temporal diffusivity change over a timeframe of 2 h (n=6). The blue circles and red diamonds represent S. aureus with and without effective gentamicin (2 μm/mL), respectively. The error bars represent standard errors. The insets are bright-field images recorded at different time points. The scale bar is 20 μm. (C) Raw images taken in the fluorescent mode. Orange microbeads represent the sensing probes and green microbeads represent references associated with the background fluctuations. The scale bar is 20 μm. (D) Effect of the rapid AST test, where a positive slope stands for an effective antibiotic on the inhibition of bacteria and vice versa. Both bacteria are sensitive to the drug concentrations used.

250x195mm (150 x 150 DPI)